

# Homology modelling of 3-oxoacyl-acyl carrier protein synthase II from *Mycobacterium tuberculosis* H37Rv and molecular docking for exploration of drugs

Vijai Singh · Pallavi Somvanshi

Received: 1 September 2008 / Accepted: 13 November 2008 / Published online: 13 December 2008  
© Springer-Verlag 2008

**Abstract** Fatty acid synthesis is essential for cell growth and viability. The 3-oxoacyl-acyl carrier protein synthase II (KAS II) from *Mycobacterium tuberculosis* catalyses initiation of the fatty acid synthesis pathway by condensation of acyl CoA and mycolic acid during the elongation phase. KAS II is a key regulator of bacterial fatty acid synthesis, and a promising target in the search for potent antibacterial drugs. Homology modelling was used to generate the 3-D protein structure using the known crystal structure, and the stereochemical quality of KAS II was validated. Effective drugs were selected that target the active amino acid residues of KAS II. The drugs thiolactomycin, thiophenone and the multidrug cerulenin isoniazid were found to be more potent for inhibition of *M. tuberculosis* due to the robust binding affinity of their protein–drug interactions. KAS II enzymes of *M. tuberculosis* and other species of *Mycobacterium* are conserved, as revealed by their close phylogenetic relationships. This study may provide new insights towards understanding the 3-D structural conformation and active amino acids of KAS II, thus providing rationale for the design of novel antibacterial drugs.

**Keywords** Drugs · Homology modelling · KAS II · Molecular docking · *Mycobacterium tuberculosis*

## Introduction

Tuberculosis (TB) is a leading infectious disease that is responsible for more than one-quarter of the world's preventable deaths [1]. The incidence of TB ranges from less than 10 per 100,000 in North America, to 100–300 per 100,000 in Asia and Western Russia, to over 300 per 100,000 in Southern and Central Africa. In total, 8 million individuals in the world develop this disease annually; due to absence of treatment, about 60% of sufferers die [2]. Antigen-based immunodiagnosis of the pathogen is an essential and primary step in the diagnosis of tuberculosis. Many proteins from *Mycobacterium tuberculosis* have been investigated as putative antigenic epitopes [3]. Although effective, vaccination and chemotherapeutic treatment takes a long time, is expensive, and, in general, is unavailable to people in many parts of the world where it is most needed.

The mycobacterial cell wall consists of unique lipids, viz. mycolic acids, very long chain fatty acids, and multimethyl branch fatty acids [4]. According to the Kyoto Encyclopedia of Genes and Genomes database [5], there are two discrete enzyme systems in the biosynthesis of fatty acids in mycobacteria: fatty acid synthase (FAS) I and II [1, 5, 6]. FAS I consists of a single polypeptide with multiple catalytic activities that creates short precursors for elongation by other fatty acids [1]. FAS II involves the biosynthesis of mycolic acids, which are major and specific long chain fatty acids of the cell envelope of *M. tuberculosis* and other *Mycobacteria* [7].

The protein MabA, also named FabG1, was recently revealed as forming part of FAS II—catalysing the NADPH-specific reduction of long chain  $\beta$ -ketoacyl derivatives, which corresponds to the second step of FAS II elongation [7]. The FAS II system includes a host of enzymes involved in the elongation of substrates bound to an acyl carrier protein to

V. Singh · P. Somvanshi (✉)  
Biotech Park,  
Sector-G Jankipuram,  
226021 Lucknow, Uttar Pradesh, India  
e-mail: psomvanshi@gmail.com

produce mycolic acids [1]. Furthermore, it has been demonstrated that the multifunctional FAS comprises the unique capability of catalysing both de novo synthesis and chain elongation of fatty acids [4]. The biosynthesis of 3-oxoacyl-acyl carrier protein synthase II (KAS II) in *M. tuberculosis* is shown in Fig. 1. Mycolic acids consist of long chain  $\alpha$ -alkyl betahydroxy fatty acids that are produced by successive rounds of elongation catalysed by a type II FAS. FAS has been identified as the major enzyme responsible for the synthesis of fatty acids in many organisms. Genes such as *AcpM* (acyl carrier protein), *kasA* ( $\beta$ -keto acyl synthase), *kasB* ( $\beta$ -keto acyl synthase), *accD6* (AcetylCoA carboxylase), *fbpc* (trehalose dimycolyl transferase), *fadE24* (fatty acylCoA dehydrogenase), *ahpc* (alkyl hydroperoxide reductase), and *efpA* (efflux protein) are responsible for fatty acid synthesis. In a recent study, we performed an in silico prediction of the putative subcellular localisation of these proteins of *M. tuberculosis* [8].

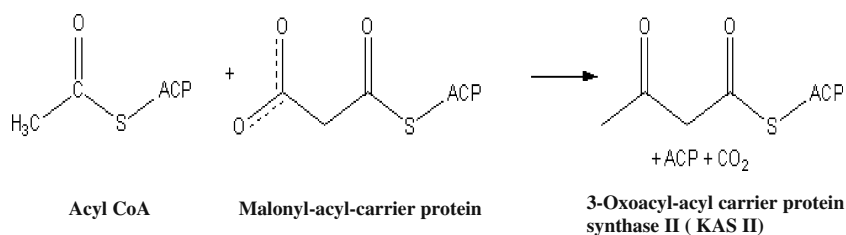
The process of fatty acid synthesis requires multiple enzyme activities of FAS systems, including  $\beta$ -keto ACP synthase (condensing enzyme),  $\beta$ -ketoACP reductase, 3OH acylACP dehydratase and enoylACP reductase. Acyl carrier protein synthase (*acpS*) catalyses the formation of holoACP, which mediates the transfer of acyl fatty acid intermediates during the biosynthesis of fatty acids and lipids [9]. The 3-D structure of KAS II of *M. tuberculosis* H37Rv has not yet been determined. KAS II is absent in humans; therefore it represents a significant potential drug target. The present study was designed to model the 3-D structure of KAS II, and to target the active amino acid residues with potential drugs. Homology between KAS II and similar proteins present in other species of *Mycobacterium* was also predicted, which revealed that the same drugs may be used to control the spread of *M. tuberculosis* and other species of *Mycobacterium*.

## Materials and methods

### Collection of sequences

The complete protein sequences of KAS II from *M. tuberculosis* H37Rv and other *Mycobacterium* species were retrieved from NCBI (<http://www.ncbi.nlm.nih.gov>).

**Fig. 1** Schematic representation of fatty acid biosynthesis in *Mycobacterium tuberculosis* H37Rv



### Blast

The relatedness of sequences deposited in databases was evaluated by BLAST [10] implemented via the NCBI server (<http://www.ncbi.nlm.nih.gov/blast>) against the complete training dataset. The BlastP (protein query–protein database) comparison was done with the protein database (PDB). The alignment with the target protein template PDB (2GP6) was performed using CLUSTAL X.

### Generation of 3-D structure through homology modelling

The crystal structure of KAS II from *M. tuberculosis* 2.40 Å resolution (PDB: 2GP6) was used as a template structure to generate the 3-D model of KAS II. The crystal 3-D structure of the template was retrieved from the PDB (<http://www.rcsb.org/pdb/>). Homology modelling was used to generate the 3-D structure of KAS II of *M. tuberculosis* H37Rv through Modeller [11] and visualisation of the 3-D structure in PYMOL [12].

### Evaluation and validation of the 3-D structure

The method applied for the evaluation of the 3-D model used the two parameters minimum model score and dope score of model and template. The 3-D structure of KAS II was validated with the programs PROCHECK [13] and WHATIF. These programs generate Ramachandran plots of the amino acid residues in the allowed region and consider the overall G-factors.

### Virtual screening of potent drugs through molecular docking

The two-dimensional structures of drugs taken from NCBI Pubchem were converted into 3-D structures using the Babel format molecule converter. The 3-D structures of KAS II and selected drugs were used for molecular docking studies. AutoDock 3.05 [14] was used to dock various drugs with the KAS II structure. The Lamarckian Genetic Algorithm (LGA) implemented in Autodock 3.0.5 was used for docking experiments. The docking parameters were as follows: 100 docking trials, population size 150, random starting position and conformational transla-

## CLUSTAL X (1.83) multiple sequence alignment

```

KAS      -----MSQPSTANG-----GFPSVVVTAVTATTSISPDIESTWKGLLAGESGIH
2GP6     MGSSHHHHHHSSGLVPRGSHMVTGKAFPYVVVTGIAMTTALATDAETTUKLLLRQSGIR
              *.   ...*          .** ****.: ***** *:* ** * :****

KAS      ALEDEFVTKWDLAVKIGGHLKDPVDSHMGRDLMRRMSYVQRMGKLLGGQLWESAGSPEVD
2GP6     TLDDPFVEEFDLPVRIGGHLLEEFDHQLTRIELRRMGYLQRMSTVLSRRLWENAGSPEVD
              :*: * ** :*: :*: ***** : . * : : :*: *:*****.:* :* :* :*****

KAS      PDRFVVVGTGLGGAERIVESYDLMNAGGPRKVSPLAVQIMPNGAAAVIGLQLGARAGV
2GP6     TNRLMVSIGTGLGSAEELVFSYDDMRARGMKAVSPLTVQKYPNGAAAVGLERHAKAGV
              .*: * :*****.*: * ** * . * * : *****: ** *****.:*: *:* **

KAS      MTPVSACSSGSEAIHAHRQIVMGDADVAVCGGVEGPIEALPIAAFSMMR-AMSTRNDEP
2GP6     MTPVSACASGAEAIARA WQQIVLGEADAAICGGVETRIEAVPIAGFAQMRIVMSTNNDDP
              *****: *: *****: *****: *****: ***** ***** *****: * :* .****: *:*

KAS      ERASRPFDKDRDGFVFGAAGALMLIETEEHAKARGAKPLARLLGAGITSDAFHVMVAPAAD
2GP6     AGACRPFDRDRDGFVFGEGGALLIETEEHAKARGANILARIMGASITSDGFHVMVAPDPN
              * .****: *****. **: *****: *****: *****: ***** * :

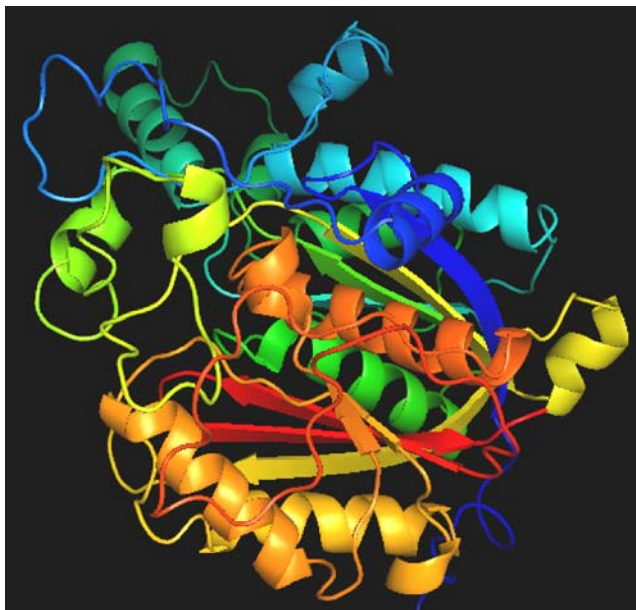
KAS      GVRAGRAMTRSLELAGLSPADIDHVNAHGTATPIGDAAEANAIR-VAGCDQAAVYAPKSA
2GP6     GERAGHAI TRAIQLAGLAPGDIDHVNAHATGTQVGDLAEGRAINNALGGNRPVYAPKSA
              * * **: *: **: :*: *: *****.* : * ** * . * . . * : : *****

KAS      LGHSIGAVGALESVLTVLTLRDGVIPPTLNYPDPEIDLDVVAGEPRYGDYRYAVNNSF
2GP6     LGHSVGA VGAVESILTVALALRDQVIPPTLNLVNLDPEIDLDVVAGEPRPGNYRYAINNSF
              *****: *****: *****: ***** ***** . ***** ***** * :*****: *****

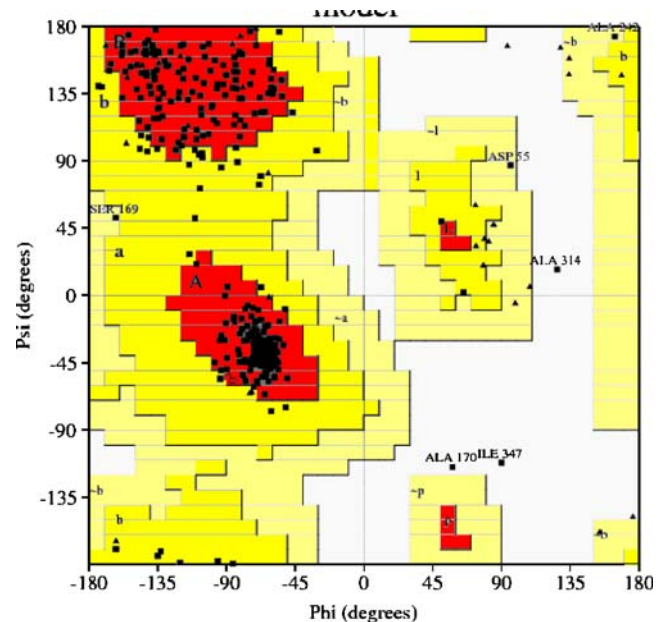
KAS      GFGGHNVALAFGRY
2GP6     GFGGHNVAIAFGRY
              *****: *****

```

**Fig. 2** Alignment of 3-oxoacyl-acyl carrier protein synthase II (KAS II) of *M. tuberculosis* H37Rv with template (PDB: 2GP6) protein sequence. Asterisks identical amino acids, dots similar amino acids



**Fig. 3** Three-dimensional (3-D) structure of KAS II from *M. tuberculosis* H37Rv ( $\alpha+\beta$ ) based on known template protein structure



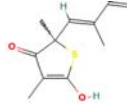
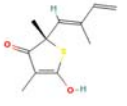
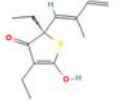

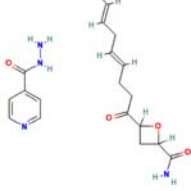
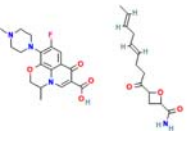
**Fig. 4** The stereochemical spatial arrangement of amino acid residues in the modelled 3-D structure of KAS II in favoured region of the Ramachandran plot

tion step ranges of 1.5 Å, rotation step ranges 35, elitism of 1, mutation rate 0.02, cross-over rate of 0.8, local search rate of 0.06 and 25 million energy evaluations. The jobs were distributed to a computer cluster. The distance-dependent function of the dielectric constant was used to calculate the energy maps and all other parameters were used at default values. Compounds with highest binding affinity from the best docked complexes were selected.

#### Construction and analysis of phylogenetic tree

The protein sequence of KAS II from *M. tuberculosis* H37Rv was used to search for homology using BLAST and homologous sequences were retrieved from the NCBI GenBank. KAS II protein sequences were aligned in CLUSTALX [15] and using the passion correction algorithm implemented in the MEGA4.0 [16] program for

**Table 1** Drugs used in this study

S. No.	CID No.	Common name of drugs	Molecular formula	IUPAC name	M.W. (g/mol)	Structure
1.	445629	Thiolactomycin	C <sub>11</sub> H <sub>14</sub> O <sub>2</sub> S	(2R)-5-hydroxy-2,4-dimethyl-2-[(1E)-2-methylbuta-1,3-dienyl]thiophen-3-one	210.29	
2.	6604034	Lopac-T-9567	C <sub>11</sub> H <sub>14</sub> O <sub>2</sub> S	(2S)-5-hydroxy-2,4-dimethyl-2-[(1E)-2-methylbuta-1,3-dienyl]thiophen-3-one	210.29	
3.	6439253	Thiotetromycin	C <sub>13</sub> H <sub>18</sub> O <sub>2</sub> S	(2R)-2,4-diethyl-5-hydroxy-2-[(1E)-2-methylbuta-1,3-dienyl]thiophen-3-one	238.34	
4.	11708239	Thiophenone	C <sub>10</sub> H <sub>14</sub> O <sub>2</sub> S	2-[(E)-but-2-enyl]-5-hydroxy-2,4-dimethylthiophen-3-one	198.28	
5.	6475077	Cerulenin & Isoniazid	C <sub>19</sub> H <sub>26</sub> N <sub>4</sub> O <sub>4</sub>	4-[(4E,7E)-nona-4,7-dienoyl]oxetane-2-carboxamide; pyridine-4-carbohydrazide	374.43	
6.	6475079	Cerulenin & floxacin	C <sub>31</sub> H <sub>39</sub> FN <sub>4</sub> O <sub>7</sub>	NA	598.66	

Note: NA; Not available.

Note: NA; Not available.

**Table 2** The interaction energy (kcal mol<sup>-1</sup>) of 3-oxoacyl-acyl carrier protein synthase II (KAS II) and drugs obtained from the molecular docking. RMS Root mean square

Drug	Binding energy (kcal mol <sup>-1</sup> )	Docked energy kcal mol <sup>-1</sup> )	Inter molecular energy kcal mol <sup>-1</sup> )	Torsional energy (kcal mol <sup>-1</sup> )	Internal energy kcal mol <sup>-1</sup> )	RMS (Å)
Cerulenin flaxacin	-07.16	-05.08	-10.90	3.74	5.82	49.40
Cerulenin isoniazid	-02.86	-06.34	-06.59	3.74	0.25	34.10
Lopac-T-2008	-06.48	-08.10	-08.35	1.87	0.25	63.06
Thiolactomycin	-06.53	-08.14	-08.40	1.87	0.25	50.70
Thiophenone	-06.22	-07.48	-08.09	1.87	0.25	63.33
Thiotetramycin	-07.10	-06.35	-09.28	2.18	2.93	39.54

construction of a phylogenetic tree by the neighbour-joining method. A total of 100 bootstrapped values were sampled to determine a measure of the support for each node on the consensus tree.

#### Protein structure accession number

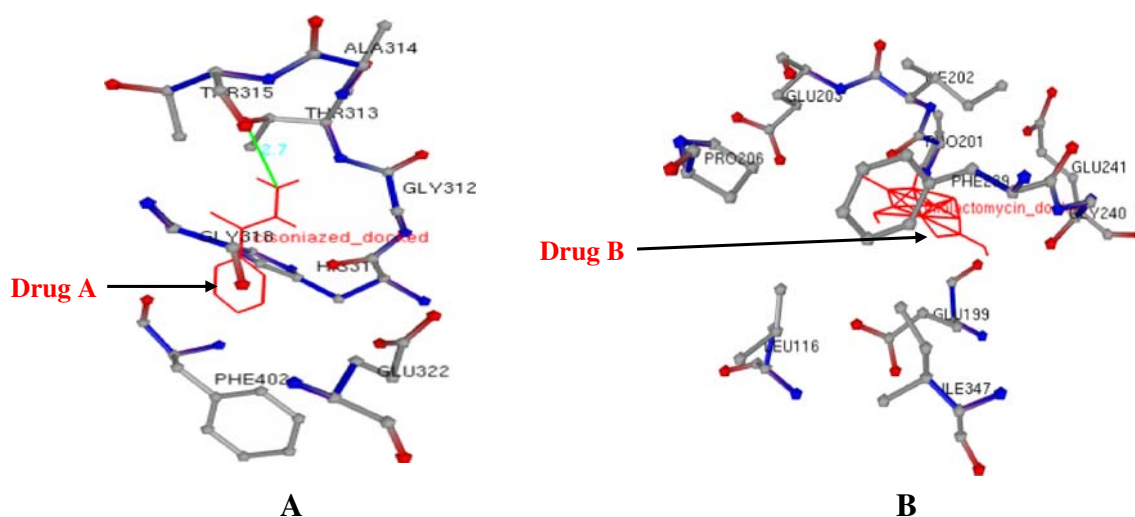
The homology model of the 3-D structure of KAS II of *M. tuberculosis* H37Rv strain was submitted to PMDB (<http://mi.caspur.it/PMDB/>) and was assigned the identifier PM0075475.

## Results and discussion

*M. tuberculosis* H37Rv is the most commonly studied laboratory strain and was first isolated in 1905 [17]. Lipids containing multiple methyl-branched fatty acids are present in the cell envelope of the pathogenic strain *M. tuberculosis*

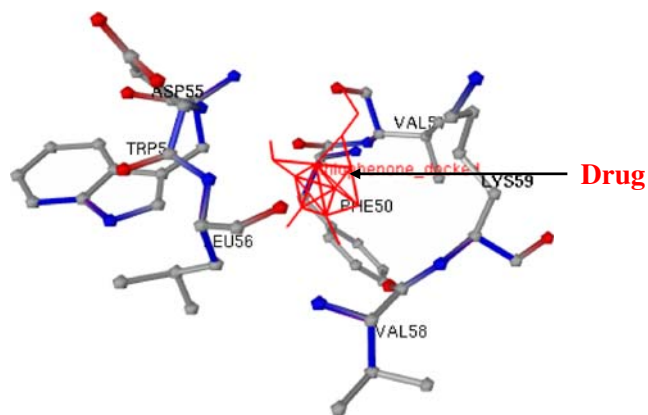
H37Rv play an important role in pathogenesis [18]. KAS II from *M. tuberculosis* H37Rv (NCBI accession no. NP\_216761.1) is 416 amino acids long and shares structural homology with the 3-D crystal structure (PDB: 2GP6) of KAS II of *M. tuberculosis*. The percentage homology between KAS II and the template was 66% identity and 79% similarity in amino acids. An alignment of KAS II from *M. tuberculosis* H37Rv with the template 3-D structure of *M. tuberculosis* (PDB: 2GP6) is shown in Fig. 2.

The protein structure was evaluated based on the free energy of KAS II and template 2GP6 3-D structure. In this study, the free energies of the 3-D structure of target and template structures were observed to be very similar. A total of five models were generated and one was selected as the 3-D model of KAS II. The energy of the 3-D structure of KAS II of *M. tuberculosis* H37Rv (43,088.06 cal/mol) closely resembles the free energy of the template crystal structure (45,123.32 cal/mol). The 3-D model structure of KAS II of *M. tuberculosis* H37Rv is



**Fig. 5** The interaction of high affinity potent drugs with KAS II of *M. tuberculosis* H37Rv. **a** KAS II with cerulenin isoniazid, **b** KAS II with thiolactomycin





**Fig. 6** The interaction of the high affinity potent drug thiophenone with KAS II of *M. tuberculosis* H37Rv

shown in Fig. 3. Eleven  $\alpha$ -helices and seven  $\beta$  sheets were obtained in the 3-D structure of KAS II, which implies that it is rich in  $\alpha$ -helix.

The stereochemical spatial arrangement matched the amino acid residues within the most favoured region in the Ramachandran plot. The torsion angles of the 3-D structure of KAS II of *M. tuberculosis* showed 87.7% of amino acid residues in the favoured region, whereas 0.9% of amino acid residues were in the disallowed region. The low percentage of amino acid residues in the disallowed region indicates the high quality of the model 3-D structure. The Ramachandran plot of the best-suited 3-D model of KAS II of *M. tuberculosis* H37Rv is shown in Fig. 4, and the overall G-factor was 1.6, which indicates the value of the favoured region for a suitable 3-D protein model. Homology modelling was used to generate the 3-D structure of  $\beta$ -ketoacyl acyl carrier synthase (KAS) III protein, which initiates the synthesis of fatty acid in *Enterococcus faecalis*. The generation of the 3-D structure was done using Modeller and the structure was validated using PROCHECK. The torsion angle of 88.9% of residues were within the allowed region and only 0.3 % of residues were in the disallowed region of the Ramachandran plot. The identification of active site residue in

this protein was performed using docking; two antibacterial drugs—Naringenin and Apigenin, which inhibit growth of bacteria [19]—were identified. Modelling was used to generate the 3-D structure of NAD<sup>+</sup> dependent DNA ligase of *M. tuberculosis*, with the 3D structure being validated by PROCHECK and WHATIF. The virtual screening of several drugs was performed via docking studies, and it was found that glycosylamines are suitable drugs with which to halt the growth of *M. tuberculosis* [20].

Table 1 lists the common name, IUPAC name, molecular formula, molecular weight and 2-D structure of each of the KAS II-specific antibacterial drugs used in this study. Six known potential drugs were selected for molecular docking against the active amino acid residues of KAS II, and three drugs, viz. cerulenin ionized complex, thiolactomycin and thiophenone, were found to have the highest binding affinity. The interaction of drugs with KAS II on the basis of docking several energies, i.e. docking energy, inter molecular energy, torsional energy, RMS and internal energy, are given in Table 2. The docking energies of the cerulenin ionized, thiolactomycin and thiophenone are  $-06.34$ ,  $-08.14$  and  $-07.48$  kcal/mol, respectively. The lowest docking energy correlated with highest binding affinity in these protein–drug interactions.

The following amino acid residues in KAS II were observed to play an active role in the interaction with the antibacterial drug cerulenin ionized: ALA314, THR315, THR313, GLY312, GLY318, HIS311, PHE402, ASP319 and GLU322. The drug was bound with these active amino acids of KAS II, and a single hydrogen bond (HB) was formed between the LIG2:H42—THR313:OG1 atom with a distance of 2.7 Å distance (Fig. 5a). The amino acid residues in KAS II active during interaction with the drug thiolactomycin these were GLU203, PRO206, ILE202, PHE239, GLU241, PRO201, GLY240, GLY200, GLU199, SER346, ILE347 and LEU116 (Fig. 5b); and those involved in interaction with Thiophenone were ASP55, VAL51, LYS59, PHE50, TRP54, LEU56 and VAL58 (Fig. 6). No HB is formed between the two drugs; a high interaction energy was found upon

**Table 3** Active amino acid residues and H-bonds formed between drugs and KAS II obtained through molecular docking

Active amino acids in KAS II	Drug	Interaction of KAS II and drug	Distance of hydrogen bonds (Å)
ALA <sub>314</sub> , THR <sub>315</sub> , THR <sub>313</sub> , GLY <sub>312</sub> , GLY <sub>318</sub> , HIS <sub>311</sub> , PHE <sub>402</sub> , ASP <sub>319</sub> , GLU <sub>322</sub>	Cerulenin ionized	LIG2:H42—THR313:OG1	2.700
GLU <sub>203</sub> , PRO <sub>206</sub> , ILE <sub>202</sub> , PHE <sub>239</sub> , GLU <sub>241</sub> , PRO <sub>201</sub> , GLY <sub>240</sub> , GLY <sub>200</sub> , GLU <sub>199</sub> , SER <sub>346</sub> , ILE <sub>347</sub> , LEU <sub>116</sub>	Thiolactomycin	ND <sup>a</sup>	ND
ASP <sub>55</sub> , VAL <sub>51</sub> , LYS <sub>59</sub> , PHE <sub>50</sub> , TRP <sub>54</sub> , LEU <sub>56</sub> , VAL <sub>58</sub>	Thiophenone	ND	ND

<sup>a</sup> Not detected

binding of drugs to the active amino acid residues in KAS II. The active amino acid residues of KAS II of *M. tuberculosis* H37Rv were identified during the docking investigation (Table 3).

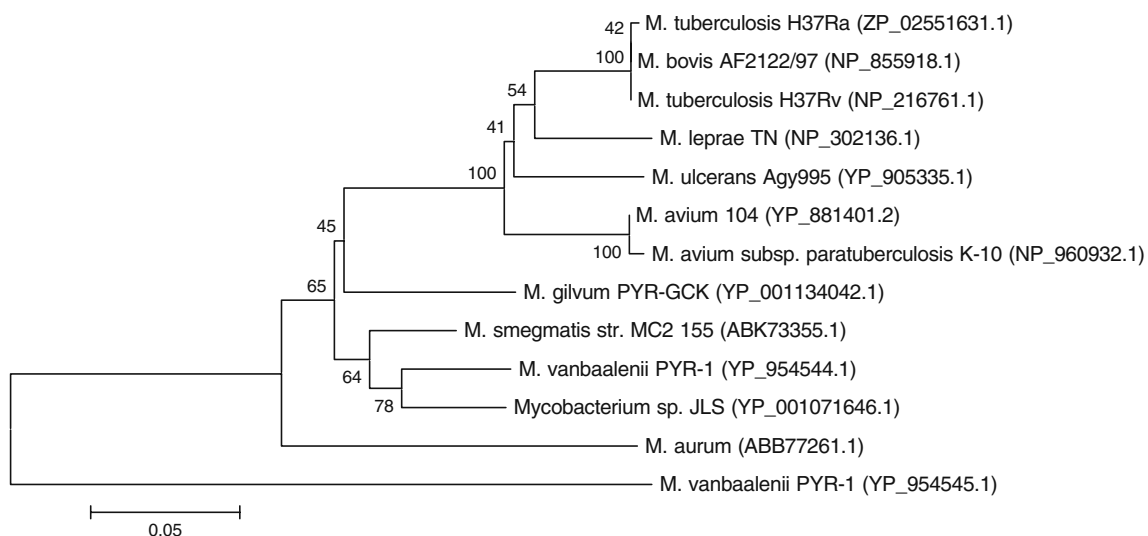
Pyridochromanones were identified by high throughput screening as potent inhibitors of NAD<sup>+</sup>-dependent DNA ligase from *Escherichia coli*. The pyridochromanones demonstrate that diverse eubacterial DNA ligases can be addressed by a single inhibitor without affecting eukaryotic ligases or other DNA-binding enzymes, which proves the value of DNA ligase as a novel target in antibacterial therapy [21]. *M. tuberculosis* codes for an essential NAD<sup>+</sup>-dependent DNA ligase (MtuLigA), which is a novel, validated, and attractive drug target. Mutants in this enzyme were created by systematically deleting domains from the C-terminal end of the enzyme to probe their functional role in the DNA nick joining reaction. Deletion of just the BRCT domain from MtuLigA resulted in total loss of activity in in vitro assays. Virtual screening and docking studies identified novel N-substituted tetracyclic indoles, which compete with NAD<sup>+</sup> and inhibit the enzyme with IC50 values in the low micromolar range [22].

A phylogenetic tree was constructed using the KAS II protein sequences of *M. tuberculosis* H37Rv and other *Mycobacterium* species. A phylogenetic tree showing the relationship between KAS II of *M. tuberculosis* and KAS II-like sequences from other species of *Mycobacterium* is shown in Fig. 7; two major clades are observed. KAS II of *M. tuberculosis* H37Rv is closely related with the KAS IIs of *M. tuberculosis* H37Ra and *M. bovis*. The same antibacterial drugs may thus be used to inhibit the growth of other species of *Mycobacterium*. These results indicate

that the drugs thiolactomycin, thiophenone, and the multidrug cerulenin isoniazid may all be useful in the inhibition of growth of closely related *Mycobacterium* species. The phylogeny indicates that KAS II is a stable and significant target for drug targeting *M. tuberculosis* H37Rv and *Mycobacterium* species.

## Conclusion

The present study was carried out to generate the 3-D structure of KAS II from *M. tuberculosis* H37Rv. A virtual screening of suitable drugs was performed, which identified thiolactomycin, thiophenone and the multidrug cerulenin isoniazid—drugs proven to result in improved inhibition of *M. tuberculosis*—and active amino acid residues, which will be useful in designing other potent drugs and drug analogs. The phylogeny of KAS II from *M. tuberculosis* indicates that the KAS II protein is conserved, suggesting that growth of other *Mycobacterium* species can be inhibited with the same drugs. This study provides new insights into the identification of drugs in the in vitro laboratory. The excessive use and abuse of antibacterial drugs has accelerated the spread of multi-drug resistant *Mycobacterium* strains. The unprecedented level of antibiotic resistance threatens to destroy drug efficacy in treating infectious diseases, posing a challenge to public health. The 3-D structure of KAS II from *M. tuberculosis* H37Rv strain and its complexes with drugs, viz. thiolactomycin, thiophenone and the multidrug cerulenin isoniazid, would need to be verified on the basis of efficacy; toxicity and pharmacokinetic properties should be validated experimentally.



**Fig. 7** Unrooted phylogenetic tree based on KAS II amino acid sequences of *M. tuberculosis* H37Rv and other related bacteria harbouring similar sequences. Bar 0.05 amino acid changes per site

## References

1. Cole ST, Brosch R, Parkhill J et al (1998) Deciphering the biology of *Mycobacterium tuberculosis* from the complete genome sequence. *Nature* 393:537–544
2. Smith I (2003) *Mycobacterium tuberculosis* pathogenesis and molecular determinants of virulence. *Clin Microbiol Rev* 16(3):463–496
3. Somvanshi P, Singh V, Seth PK (2008) In silico prediction of epitopes in virulence proteins of *Mycobacterium tuberculosis* H37Rv for diagnostic and subunit vaccine design. *J Proteomics Bioinform* 1:143–153
4. Kikuchi S, Rainwater DL, Kolattukudy PE (1992) Purification and characterization of an unusually large fatty acid synthase from *Mycobacterium tuberculosis* var. *bovis* BCG. *Arch Biochem Biophys* 295:318–326
5. Kanehisa M, Goto S, Kawashima S et al (2002) The KEGG databases at GenomeNet. *Nucleic Acids Res* 30:42–46
6. Kolattukudy PE, Fernandes ND, Azad AK et al (1997) Biochemistry and molecular genetics of cell-wall lipid biosynthesis in mycobacteria. *Mol Microbiol* 24:263–270
7. Ducasse-Cabanot S, Cohen-Gonsaud M, Marrakchi H et al (2004) In vitro inhibition of the *Mycobacterium tuberculosis* beta-ketoacyl-acyl carrier protein reductase MabA by isoniazid. *Antimicrob Agents Chemother* 48:242–249
8. Somvanshi P, Singh V, Seth PK (2008) In silico analysis of subcellular localization of putative proteins of *Mycobacterium tuberculosis* H37Rv strain. *The Internet Journal of Health* 7(1)
9. Chopra S, Singh SK, Prasad S et al (2002) Expression, purification, crystallization and preliminary X-ray analysis of the acyl carrier protein synthase (acpS) from *Mycobacterium tuberculosis*. *Acta Cryst D* 58:179–181
10. Altschul SF, Thomas LM, Alejandro AS et al (1997) Gapped BLAST and PSI-BLAST: a new generation of protein database search programs. *Nucleic Acids Res* 25:3389–3402
11. Sali A, Blundell TL (1993) Comparative protein modeling by satisfaction of spatial restraints. *J Mol Biol* 234:779–815
12. Delano WL (2002) The PYMOL molecular graphics system. Palo Alto CA
13. Laskowski RA, MacArthur MW, Moss DS et al (1993) PROCHECK: a program to check the stereochemical quality of protein structure. *J Appl Crystallogr* 26:283–291
14. Morris GM, Goodsell DS, Halliday RS et al (1998) Automated docking using a Lamarckian genetic algorithm and an empirical binding free energy function. *J Comp Chem* 19:1639–1662
15. Thompson JD, Gibson TJ, Plewniak F et al (1997) The CLUSTALX windows interface: flexible strategies for multiple sequence alignment aided by quality analysis tools. *Nucleic Acids Res* 25:4876–4882
16. Tamura K, Dudley J, Nei M et al (2007) MEGA4: Molecular Evolutionary Genetics Analysis (MEGA) software version 4.0. *Mol Biol Evol* 24:1596–1599
17. Jacobs W, Brennan P, Curlin G et al (1996) Comparative sequencing. *Science* 274:17–18
18. Rousseau C, Turner OC, Rush E et al (2003) Sulfolipid deficiency does not affect the virulence of *Mycobacterium tuberculosis* H37Rv in mice and guinea pigs. *Infect Immun* 71(8):4684–4690
19. Jeong KW, Lee JY, Kim Y (2007) Homology modeling and docking study of beta-ketoacyl acyl carrier protein synthase III from *Enterococcus faecalis*. *Bull Korean Chem Soc* 28(8):1335–1340
20. Srivastava SK, Dube D, Tewari N et al (2005) *Mycobacterium tuberculosis* NAD<sup>+</sup> dependent DNA ligase is selectively inhibited by glycosylamines compared with human DNA ligase I. *Nucleic Acids Res* 33(22):7090–7101
21. Brotz-Oesterhelt H, Knezevic I, Bartel S et al (2003) Specific and potent inhibition of NAD<sup>+</sup>-dependent DNA ligase by pyridochromanones. *J Biol Chem* 278(41):39435–39442
22. Srivastava SK, Dube D, Kukshal V et al (2007) NAD<sup>+</sup> -dependent DNA ligase (Rv3014c) from *Mycobacterium tuberculosis*: novel structure-function relationship and identification of a specific inhibitor. *Proteins* 69(1):97–111